Separation Science and Technology
Publication details, including instructions for authors and subscription information:
http://www.informaworld.com/smpp/title~content=t713708471

DESORPTION KINETIC MODEL FOR SUPERCRITICAL FLUID EXTRACTION OF SPEARMINT LEAF OIL

Kyoung Heon Kim[a][b]; Juan Hong[a]
[a] Department of Chemical and Biochemical Engineering and Materials Science, University of California, Irvine, California, U.S.A. [b] National Renewable Energy Laboratory, CO, U.S.A.

To cite this Article Kim, Kyoung Heon and Hong, Juan(2001) 'DESORPTION KINETIC MODEL FOR SUPERCRITICAL FLUID EXTRACTION OF SPEARMINT LEAF OIL', Separation Science and Technology, 36: 7, 1437 — 1450
To link to this Article: DOI: 10.1081/SS-100103880
URL: http://dx.doi.org/10.1081/SS-100103880

SEPARATION SCIENCE AND TECHNOLOGY, 36(7), 1437–1450 (2001)

DESORPTION KINETIC MODEL FOR SUPERCRITICAL FLUID EXTRACTION OF SPEARMINT LEAF OIL

Kyoung Heon Kim* and Juan Hong

Department of Chemical and Biochemical Engineering and
Materials Science, University of California, Irvine,
California 92697

ABSTRACT

To characterize the dynamic behavior in supercritical CO_2 extraction of essential oil components (carvone and limonene) from spearmint leaves under pressures of 69.0 bar (near-critical), 84.5 bar (supercritical), and 103.4 bar (supercritical) and temperatures of 39 and 49°C, a simplified desorption kinetic model was developed. In the desorption model, a linear irreversible desorption kinetics was assumed, and the releasing rate of oil components from the leaf particle matrix was defined by a desorption rate constant as a model fitting parameter. Despite the simplicity of the desorption kinetic model, the experimental data and the predicted values by the desorption kinetic model were in good agreement. In the present study, the desorption rate constant mostly increased as the CO_2 flow rate and pressure were increased and as the temperature and leaf particle size were decreased.

Key Words: Supercritical carbon dioxide; Extraction; Desorption kinetics; Spearmint oil.

---

*Corresponding author. National Renewable Energy Laboratory, 1617 Cole Boulevard, Golden, CO 80401. Fax: (303) 384-6827; E-mail: khekim@nrel.gov

INTRODUCTION

Supercritical CO_2 extraction has received much attention for its potential applications in the food and pharmaceutical industries. Most supercritical fluid extractions using natural materials have been limited to laboratory-scale operations. So far, few processes, such as the decaffeination of coffee beans, have been extended to commercial scale. The difficulty in scale-up is partly due to a lack of understanding about the extraction behavior in the supercritical fluid extraction (SFE) of real materials. While many studies on supercritical fluids (SCFs) have focused on the thermodynamic aspect, less attention has been paid to kinetics in SFE. From an industrial viewpoint, knowing about both extraction kinetics and thermodynamics is important, since in the SFE of real substrates the solubility behavior is found to be only one of several important factors (1).

In the SFE of plant materials, compared with the number of SFEs performed on plant seeds (2–14), relatively few extraction kinetic and mass transfer studies have been performed on herbaceous materials (15–19). The supercritical CO_2 (SC-CO_2) extraction of herbaceous materials generally results in a lower oil yield and a more complex final product profile (15,17–19) than that of plant oil seeds. In the herbaceous substrate extraction, the mass transfer of solute may be more affected by the interaction of solute with complex inner matrix of herbaceous substrates, as well as the interactions between different solutes, than by the solubility of solute in the fluid phase.

The herbaceous materials are complex in terms of geometry, solute distribution, and matrix structure. The application of internal diffusion and external mass transfer models to the SFE of herbaceous materials is not satisfactory despite the difficulty in obtaining their solutions, since it gives unreasonably low estimates of internal diffusion coefficients as found in previous studies (17,18,20,21). Moreover, from an engineering viewpoint, a simplified model is preferred to an exact but complicated model. By applying the heat transfer analogy of a hot ball in a uniform medium to the mass transfer, Bartle et al. (22) proposed a simple SFE model that only takes into account the internal mass transfer resistance. In the SC-CO_2 extraction of peppermint leaves, the desorption of essential oil from lipid materials existing in the leaf matrix was found to be the rate–controlling step in the entire extraction process (15).

The objective of this study was to develop and evaluate a simplified desorption kinetic model for the SFE of essential oil components—carvone and limonene—from spearmint leaves. The effects of pressure, temperature, CO_2 flow rate, and leaf particle size on the desorption rate were also investigated. Therefore, estimated parameters can be used to predict the extraction behavior of similar systems with the desorption model in the same range of extraction conditions used in this study.

EXPERIMENTAL SECTION

Spearmint leaves, a local product obtained from southern California, were washed with deionized water to remove dirt and air–dried at room temperature for one week. They were then cut into pieces with an average radius of 0.15 mm. The cut spearmint leaf particles were homogeneously mixed and then stored in a desiccator. When fine particle sized leaves were needed, the cut leaves were ground using a mortar and pestle and the average radius of the ground leaf particles was reduced to 0.03 mm.

The particle sizes of the above leaf particles were measured with USA Standard Testing Sieves. The apparent density of spearmint leaf particles was measured by shortly immersing leaf particles in ethanol (99.9%) and immediately measuring the total volume increase. To calculate the porosity of the leaf particles, the solid density of completely ground leaves (particle size smaller than 0.001 mm) was measured. Both the apparent density of leaf particles and the solid density of the ground leaves were used in calculating the leaf porosity by the method used by Goto et al. (15).

CO_2 at 99.6% or 99.9% purity was used for extraction. Methanol (99.9% purity) was used as a collection solvent. Spearmint leaf particles (2 g) were placed with glass beads (2 mm diameter) in the extraction vessel (50 cm^3 internal volume, Valco, Houston, TX). Extraction was performed by using a supercritical fluid controller and delivery system (Computer Chemical System, Unionville, NJ). The total contents of carvone and limone in the spearmint leaves were determined by carrying out SFE in duplicate at 39°C and 103.4 bar for 1500 min. These oil contents were used to estimate the initial oil concentration of spearmint leaf particles. The detailed description of the extraction apparatus and experimental procedure was reported previously (16).

RESULTS AND DISCUSSION

Development of the Desorption Kinetic Model

Entering the extractor at a constant flow is SC-CO_2, and leaving at the same flow rate is the SC-CO_2 solution containing extracted essential oil components. The slow mass flow rate of CO_2 compared to the large void volume of packed bed in the extractor rendered the following assumptions: the essential oil concentration in the bulk fluid of the extractor is uniform and the fluid temperature is constant. Using the analogy of spearmint leaves to peppermint leaves which showed the desorption–controlled extraction rate (15), it was assumed that the oil faced no additional mass transfer resistance once the oil was desorbed from leaf matrix to the CO_2 phase, regardless of whether it was in the leaf pores or in the bulk fluid.

Release of essential oil components from the plant matrix is specified by the desorption rate constant, *k*. Due to a lack of information about the adsorption isotherm equilibrium, the irreversible linear desorption kinetics was used on the mass balance of oil components in leaf particles as in Eq. (1). $\bar{c}$ is the concentration of solute inside pores of leaf particles, *W* is the weight of leaf particles per extraction, α is the void fraction of leaf particles, and ρ_p is the apparent density of leaf particles.

$$\frac{\mathrm{d}\left(\alpha \frac{W}{\rho_p} \bar{c}\right)}{\mathrm{d}t} = -k_e \alpha \frac{W}{\rho_p} \bar{c} \tag{1}$$

The bulk fluid mass balance for essential oil components in the extractor is written as Eq. (2). The essential oil components desorbed from the leaf matrices are instantaneously carried away by the bulk fluid. The bulk fluid with a solute concentration *C* leaves the extractor with the void volume *V* at the constant flow rate *q*.

$$\frac{\mathrm{d}(VC)}{\mathrm{d}t} = \frac{\mathrm{d}\left(\alpha \frac{W}{\rho_p} \bar{c}\right)}{\mathrm{d}t} - qC \tag{2}$$

The initial oil concentration in the bulk fluid is zero, and the initial oil concentration inside leaf particles is expressed as $\bar{c}_0$. Therefore, the following boundary conditions are obtained:

$$C = 0 \quad \text{at} \quad t = 0 \tag{3}$$

$$\bar{c} = \bar{c}_0 \quad \text{at} \quad t = 0 \tag{4}$$

Let

$$\alpha \frac{W}{\rho_p} = V_p \tag{5}$$

where V_p is the total pore volume inside leaf particles packed in the extractor.

By integrating Eq. (1), we find the concentration of oil in the leaf particles to be:

$$\bar{c} = \bar{c}_0 e^{-kt} \tag{6}$$

To find the variation of oil concentration in the bulk fluid with time, the oil concentration in leaf particles from Eq. (6) is substituted into Eq. (2) governing the rate of oil mass change in the bulk fluid. Thus,

$$\frac{\mathrm{d}C}{\mathrm{d}t} = k\left(\frac{V_p}{V}\right)\bar{c}_0 e^{-kt} - \frac{q}{V} C \tag{7}$$

The above first-order linear differential equation can be solved by introducing an integrating factor, exp(qt/V). The integration results in the following:

$$Ce^{\frac{q}{V}t} = \frac{\left(\frac{V_p}{V}\right)k\bar{c}_0}{\left(\frac{q}{V} - k\right)} e^{\left(\frac{q}{V} - k\right)t} + \text{constant} \tag{8}$$

By using the initial condition, $C = 0$ at $t = 0$, we find the constant to be:

$$\text{constant} = \frac{\left(\frac{V_p}{V}\right)k\bar{c}_0}{} \tag{9}$$

The final solution is obtained as Eq. (10), which shows the oil concentration change in the bulk fluid over time.

$$C = \bar{c}_0 \frac{Vp}{V} k \left(\frac{e^{-kt}}{\frac{q}{V} - k} + \frac{e^{-\frac{q}{V}t}}{k - \frac{q}{V}} \right) \tag{10}$$

Prediction by the Desorption Kinetic Model

Table 1 shows various parameters used in prediction by the desorption kinetic model. The densities of CO_2 at experimental conditions were calculated by Altunin–Gadeskii equation of state (23). The desorption kinetic model was fitted to the extraction data for the oil concentration in the bulk fluid (C) by optimizing the desorption rate constant, k. Nonlinear regression was carried out using a scientific graphing software SigmaPlot® for PC (Jandel Scientific Co., Chicago, IL)

Table 1. Parameters Used in the Prediction by the Desorption Kinetic Model

Property	Value
Average radius of leaf particle (R)	1.52×10^{-2} (cm)
Apparent density of leaf particle (ρ_p)	1.11 (g/cm^3)
Porosity of leaf particle (α)	0.333
Initial concentration of carvone in pores of leaf particles ($\bar{c}_0$)	8.25×10^{-3} (g/cm^3)
Initial concentration of limonene in pores of leaf particles ($\bar{c}_0$)	3.60×10^{-3} (g/cm^3)
Total void volume of the packed extractor (V)	16.2 (cm^3)
Mass of leaf particles per extraction (W)	2.0 (g)

to optimize the constant, k. The oil concentration in the bulk fluid, C was then calculated using optimal k values on each extraction condition. The cumulative mass of oil components was obtained by integrating the oil concentration over time. Both the concentration of oil in the bulk fluid and the cumulative mass of oil components were compared with the experimental data in the figures.

Effect of Temperature

The temperature effects at 69.0 bar (near-critical) and at 84.5 bar (supercritical) are shown in Figs. 1 and 2, respectively. Table 2 lists the estimated

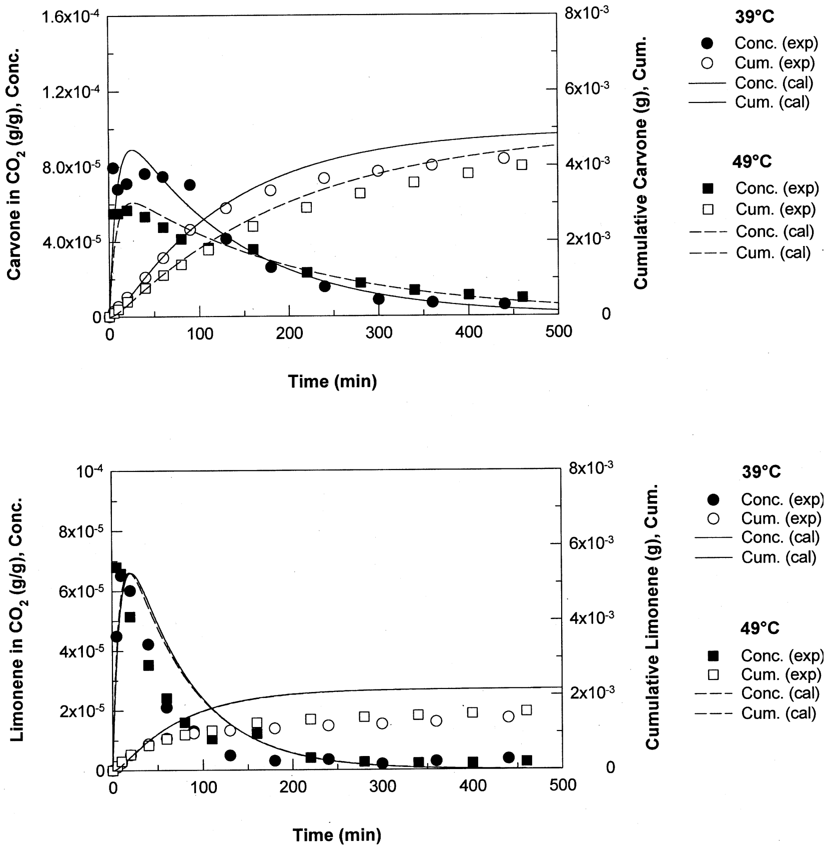

Figure 1. Comparison of oil concentration in bulk fluid (Conc.) and cumulative mass of oil components (Cum.) between experimental data and predicted curves by the desorption kinetic model for the effect of temperature on carvone and limonene extraction at 69.0 bar.

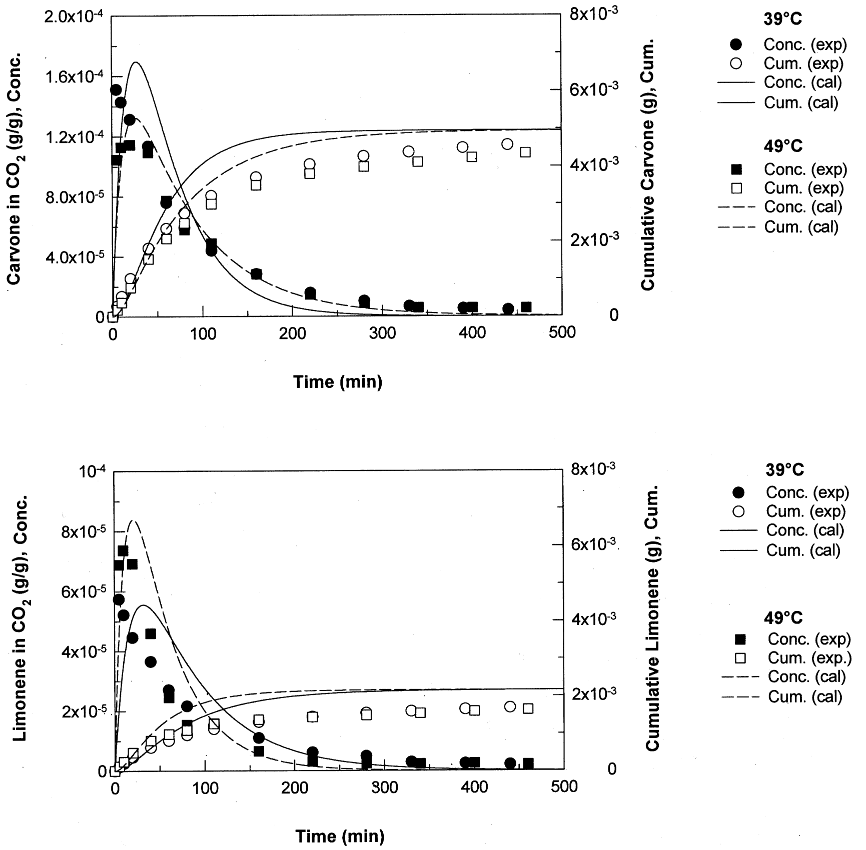

Figure 2. Comparison of oil concentration in bulk fluid (Conc.) and cumulative mass of oil components (Cum.) between experimental data and predicted curves by the desorption kinetic model for the effect of temperature on carvone and limonene extraction at 84.5 bar.

Table 2. Effects of Temperature and Pressure on the Desorption Rate Constant in Extraction of Carvone and Limonene

T (°C)	P (bar)	k (min^{-1}) Carvone	Limonene
39	69.0	7.71×10^{-3}	1.46×10^{-2}
39	84.5	2.18×10^{-2}	1.43×10^{-2}
39	103.4	5.74×10^{-2}	7.04×10^{-2}
49	69.0	4.95×10^{-3}	1.42×10^{-2}
49	84.5	1.33×10^{-2}	2.18×10^{-2}
49	103.4	2.38×10^{-2}	2.71×10^{-2}

desorption rate constants at different temperatures and pressures. As in the experimental data, faster extraction rates were predicted at lower temperatures at both pressures in the carvone extraction. Thermodynamically, a lower temperature at a fixed pressure results in a higher density of CO_2 than at a higher temperature at the same pressure. The SC-CO_2 of a higher density thus renders a higher solubility to solute as seen in the equilibrium solubility study of spearmint oil components in SC-CO_2 (1). Therefore, the faster extraction rate of carvone at 39°C than at 49°C is attributable to the higher solubility of carvone in SC-CO_2 at 39°C. However, the extraction rates of limonene at 69.0 bar were similar at 39°C and at 49°C, thereby giving the similar desorption rate constants. The lower initial concentration of limonene in leaf pores and the higher equilibrium solubility of limonene than carvone (1) may account for the insignificant temperature effect on the limonene extraction.

Effect of Pressure

Figure 3 displays the effect of pressure in the extractions carried out at 49°C. The effect of pressure was more pronounced in the carvone extraction than in the limonene extraction, showing a significantly higher extraction rate at a higher pressure. Accordingly, the desorption rate constants became larger with an increase in pressure. The magnitude of increase of extraction rate with increasing pressure was much higher when pressure was increased from 69.0 bar (near-critical) to 84.5 bar (supercritical) than when it was increased from 84.5 bar to 103.4 bar (supercritical). This may be explained by the abrupt increase of solute solubility in the fluid phase near the critical point of CO_2. As seen in Table 2, the desorption rate constant generally increased with increasing pressure. This result is in accordance with increased solubility at a higher pressure due to a higher density of CO_2 at a higher pressure. The similar trend has been observed in desorption of ethyl acetate from activated carbon (24).

Effect of CO_2 Flow Rate

Figure 4 illustrates the comparison between extraction data and prediction curves for the effect of CO_2 flow rate at 39°C and 84.5 bar. The desorption rates for both carvone and limonene increased with an increase in CO_2 flow rate, thus exhibiting a more rapid increase in cumulative mass curve at a higher flow rate. The oil concentration in bulk fluid was kept lower at a higher flow rate. In terms of extraction efficiency (i.e., g solute extracted/g CO_2 used), a higher CO_2 flow rate gave a lower extraction efficiency as we know from the cumulative mass curve, of which slope did not increase by the ratio of CO_2 flow rate increase. As

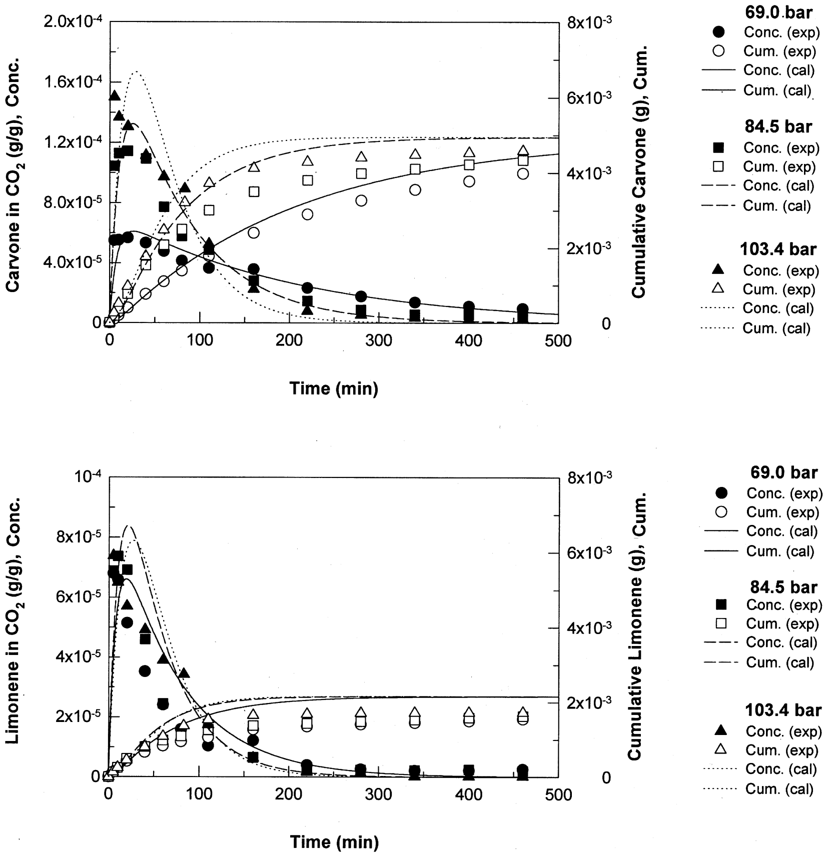

Figure 3. Comparison of oil concentration in bulk fluid (Conc.) and cumulative mass of oil components (Cum.) between experimental data and predicted curves by the desorption kinetic model for the effect of pressure on carvone and limonene extraction at 49°C.

shown in Table 3, the desorption rate constants for carvone and limonene increased with an increase in CO$_2$ flow rate.

Effect of Leaf-Particle Size

The experimental data and prediction curves for the extraction of spearmint leaves with different particle sizes are shown in Fig. 5. With the smaller particle size, a higher carvone concentration was observed in the initial extraction period; hence, the slope of the cumulative amount curve became steeper. Accordingly, the desorption rate constant was higher for the smaller leaf–particle size as listed in

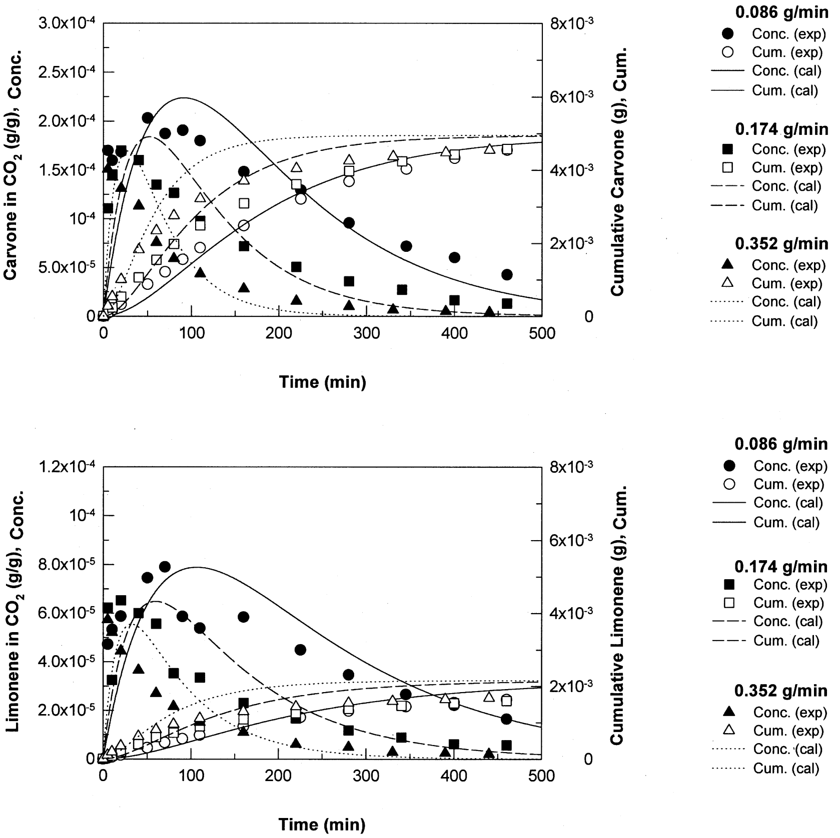

Figure 4. Comparison of oil concentration in bulk fluid (Conc.) and cumulative mass of oil components (Cum.) between experimental data and predicted curves by the desorption kinetic model for the effect of CO$_2$ flow rate on carvone and limonene extraction at 39°C and 84.5 bar.

Table 3. Effects of CO$_2$ Flow Rate and Leaf-Particle Size on the Desorption Rate Constant in Carvone Extraction at 39°C and 84.5 Bar

Mass Flow Rate of CO$_2$ (g/min)	Radius of Leaf Particles (cm)	k (min^{-1}) Carvone	k (min^{-1}) Limonene
0.086	1.52×10^{-2}	8.31×10^{-3}	5.87×10^{-3}
0.174	1.52×10^{-2}	1.22×10^{-2}	8.85×10^{-3}
0.352	1.52×10^{-2}	2.18×10^{-2}	1.43×10^{-2}
0.168	2.50×10^{-3}	2.91×10^{-2}	—

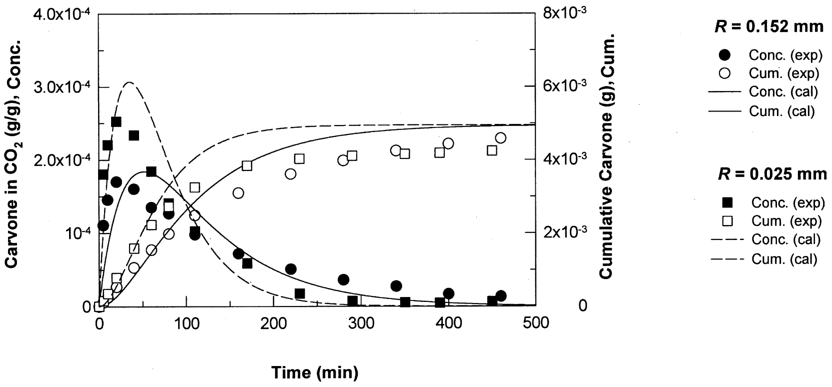

Figure 5. Comparison of oil concentration in bulk fluid (Conc.) and cumulative mass of oil components (Cum.) between experimental data and predicted curves by the desorption kinetic model for the effect of leaf-particle size on carvone extraction at 39°C and 84.5 bar.

Table 3. Therefore, the smaller particle size was more effective for the rapid carvone extraction. However, the final yield of limonene in the extraction of the smaller particles was lower than that of the larger particles, probably due to the loss of limonene in the grinding process for making the smaller leaf particles, as reported by others (15).

Effect of Ethanol Modifier

Figure 6 summarizes the effect of an ethanol modifier. Mainly, the addition of ethanol to leaf particles prior to extraction as a modifier to SC-CO_2 did not result in significant differences in extraction behavior regardless of the amounts of ethanol added. The addition of 0.5 g ethanol caused the fastest carvone extraction, thus giving the highest desorption rate constant as seen in Table 4. Meanwhile, the

Table 4. Effect of Ethanol Modifier to CO_2 on the Desorption Rate Constant in Extraction of Carvone and Limonene at 39°C and 84.5 Bar

	k (min^{-1})	
Ethanol Added (g)	Carvone	Limonene
0.0	1.22×10^{-2}	8.85×10^{-3}
0.2	1.41×10^{-2}	3.11×10^{-2}
0.5	1.46×10^{-2}	1.37×10^{-2}
3.0	1.12×10^{-2}	9.63×10^{-3}

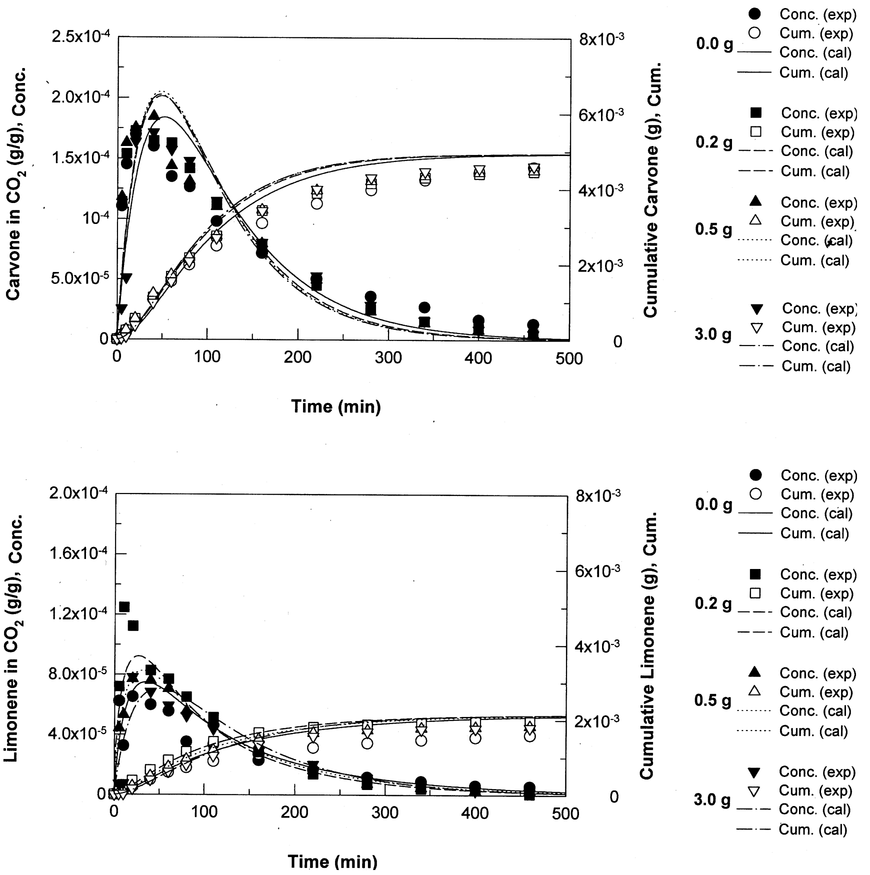

Figure 6. Comparison of oil concentration in bulk fluid (Conc.) and cumulative mass of oil components (Cum.) between experimental data and predicted curves by the desorption kinetic model for the effect of ethanol modifier on carvone and limonene extraction at 39°C and 84.5 bar.

most rapid extraction of limonene resulting in the highest desorption rate constant for limonene was observed with the 0.2 g ethanol addition.

CONCLUSIONS

The dynamic behavior of essential oil components (carvone and limonene) extraction from spearmint leaves was well–predicted by a simplified desorption kinetic model. In general, the desorption rate constant increased with an increase in extraction pressure and CO_2 flow rate and with a decrease in extraction temperature. Although the desorption model did not enable the complete understanding of the spearmint oil extraction behavior, the estimation of the desorption constant may be useful for predicting extraction curves for the similar solute–solvent system within the range of conditions used in the present work.

ACKNOWLEDGMENTS

The authors express their gratitude to the grant support of the University of California Energy Institute and the Monsanto Co.

REFERENCES

1. Kim, K. H.; Hong, J. Equilibrium solubilities of spearmint oil components insupercritical carbon dioxide. Fluid Phase Equilib. **1999**, *164*, 107–115.
2. Bernardo-Gil, M. G. *Extraction of rape-seed oil using compressed CO_2: evaluation of mass transfer coefficients*. Proceedings of the International Symposium on Supercritical Fluids, Nice, France, 1988, 651–656.
3. Bully, N. R.; Fattori, M.; Meisen, A.; Moyls, L. Supercritical fluid extraction of vegetable oil seeds. J. Am. Oil Chem. Soc. **1984**, *61*, 1362–1365.
4. Cocero, M. J.; Calvo, L. Supercritical fluid extraction of sunflower seed oil with CO_2-ethanol mixtures. J. Am. Oil Chem. Soc. **1996**, *73*, 1573–1578.
5. Cuperus, F. P.; Boswinkel, G.; Muuse, B. G.; Derksen, J. T. P. Supercritical carbon dioxide extraction of Dimorphoteca pluvialis oil seeds. J. Am. Oil Chem. Soc. **1996**, *73*, 1675–1679.
6. Gomez, A. M.; Ropez, C. P. and de la Ossa, E. M. Recovery of grape seed oil by liquid and supercritical carbon dioxide extraction: a comparison with conventional solvent extraction. Chem. Eng. J. **1996**, *61*, 227–231.
7. Lancas, F. M.; Queiroz, M. E. C.; da Silva, I. C. E. Seed oil extraction with supercritical carbon dioxide modified with pentane. Chromatogr. **1994**, *39*, 687–692.
8. Lee, A. K. K.; Bulley, N. R.; Fattori, M.; Meisen, A. Modelling of supercritical carbon dioxide extraction of canola oilseed in fixed beds. J. Am. Oil Chem. Soc. **1986**, *63*, 921–925.
9. Manninen, P.; Parkarianen, J.; Kallio, H. Large-scale supercritical carbon dioxide extraction and supercritical carbon dioxide countercurrent extraction of cloudberry seed oil. J. Agric. Food Chem. **1997**, *45*, 2533–2538.
10. Perrut, M.; Clavier, J. Y.; Poletto, M.; Reverchon, E. Mathematical modeling of sunflower seed extraction by supercritical CO_2. Ind. Eng. Chem. Res. **1997**, *36*, 430–435.

11. Reverchon, E.; Osseo, L. S. Comparison of processes for the supercritical carbon dioxide extraction of oil from soybean seeds. J. Am. Oil Chem. **1994**, *71*, 1007–1012.
12. Roy, B. C.; Goto, M.; Hirose, T.; Navaro, O.; Hortacsu, O. Extraction rates of oil from tomato seeds with supercritical carbon dioxide. J. Chem. Eng. Jpn. **1994**, *27*, 768–772.
13. So, G. C.; Macdonald, D. G. Kinetics of oil extraction from canola (rapeseed). Can. J. Chem. Eng. **1986***, 64*, 80–86.
14. Tolboe, O.; Hansen, I. R.; Shukla, V. K. S. *Extraction of oil from evening primrose seed.* Proceedings of the 1st International Symposium on Supercritical Fluids, Nice, France, 1988, 685–690.
15. Goto, M.; Sato, M.; Hirose, T. Extraction of peppermint oil by supercritical carbon dioxide. Chem. Eng. Jpn. **1993**, *26*, 401–407.
16. Kim, K. H.; J. Hong, J. Dynamic extraction of spearmint oil components by using supercritical CO_2. Sep. Sci. Technol. **2000***, 35*, 315–322.
17. Reverchon, E.; Osseo, L. S.; Gorgoglione, D. Supercritical CO_2 extraction of basil oil: characterization of products and process modeling. J. Supercrit. Fluids **1994***, 7*, 185–190.
18. Reverchon, E.; Donsi, G.; Osseo, L. S. Modeling of supercritical extraction from herbaceous matrices. Ind. Eng. Chem. Res. **1993**, *32*, 2721–2726.
19. Ozer, E. O.; Platin, S.; Akman, U.; and Hortacsu, O. Supercritical carbon dioxide extraction of spearmint oil from mint-plant leaves. Can. J. Chem. Eng. **1996**, *74*, 920–928.
20. King, J. W.; Cygnarowicz-Provost, M.; Favati, F. Supercritical fluid extraction of evening primrose oil kinetic and mass transfer effects. Ital. J. Food Sci. **1997**, *9*, 193–204.
21. Nguyen, K.; Barton, P.; Spencer, J. S. Supercritical carbon dioxide extraction of vanilla. J. Supercrit. Fluids **1991**, *4*, 40–46.
22. Bartle, K. D.; Clifford, A. A.; Hawthorne, S. B.; Langenfeld, J. J.; Miller, D. J.; Robinson, R. A model for dynamic extraction using a supercritical fluid. J. Supercrit. Fluids **1990***, 3*, 143–149.
23. Angus, S.; Armstrong, B.; de Reuck, K. M.; Altunin, V. V.; Gadeskii, O. G.; Chapela, A.; Rowlinson, J. S. *International Thermodynamic Tables of the Fluid State Carbon Dioxide*; Pergamon Press: Oxford, 1976.
24. Srinivasan, M.; Smith, J. M.; McCoy, B. J. Supercritical fluid desorption from activated carbon. Chem. Eng. Sci. **1990**, *45*, 1885–1895.

Received May 2000
Revised August 2000

Downloaded At: 10:47 25 January 2011

Request Permission or Order Reprints Instantly!

Interested in copying and sharing this article? In most cases, U.S. Copyright Law requires that you get permission from the article's rightsholder before using copyrighted content.

All information and materials found in this article, including but not limited to text, trademarks, patents, logos, graphics and images (the "Materials"), are the copyrighted works and other forms of intellectual property of Marcel Dekker, Inc., or its licensors. All rights not expressly granted are reserved.

Get permission to lawfully reproduce and distribute the Materials or order reprints quickly and painlessly. Simply click on the "Request Permission/Reprints Here" link below and follow the instructions. Visit the U.S. Copyright Office for information on Fair Use limitations of U.S. copyright law. Please refer to The Association of American Publishers' (AAP) website for guidelines on Fair Use in the Classroom.

The Materials are for your personal use only and cannot be reformatted, reposted, resold or distributed by electronic means or otherwise without permission from Marcel Dekker, Inc. Marcel Dekker, Inc. grants you the limited right to display the Materials only on your personal computer or personal wireless device, and to copy and download single copies of such Materials provided that any copyright, trademark or other notice appearing on such Materials is also retained by, displayed, copied or downloaded as part of the Materials and is not removed or obscured, and provided you do not edit, modify, alter or enhance the Materials. Please refer to our Website User Agreement for more details.

Order now!

Reprints of this article can also be ordered at

http://www.dekker.com/servlet/product/DOI/101081SS100103880